Gonzalez-Ausejo, J.; Cabedo Mas, L.; Gámez-Pérez, J.; Mollá Romano, S.; Giménez Torres, E.; Compañ Moreno, V. (2015). Modification of Nafion Membranes with Polyaniline to Reduce Methanol Permeability. Journal of The Electrochemical Society. 162(14):E325-E333. doi:10.1149/2.0521514jes.

Modification of Nafion® membranes with polyaniline to reduce methanol permeability

J. Gonzalez-Ausejo [1], L. Cabedo[1], J.Gámez-Pérez[1], S. Mollá[2], E. Giménez[3], V. Compañ[2 *]

1. Polymers and Advanced Materials Group (PIMA), Universitat Jaume I, 12071, Castellón, Spain.

2. Departamento de Termodinámica Aplicada. Universidad Politécnica de Valencia. 46022-Valencia Spain

3. Instituto de Tecnología de Materiales, Universidad Politécnica de Valencia, 46022, Valencia. Spain.

Corresponding author e-mail: vicommo@ter.upv.es

Highlights

1. Nafion® membranes with polyaniline (PAni) to reduce methanol crossover has been studied.

2. The PAni polymerization is done by two different routes: immersion and crossover

3. The oxidation state of the polyaniline to emeraldine is bigger for the crossover route.

4. Crossover route is more effective for decreasing of the methanol permeability.

5. The performances of membranes assembly prepared with PAni were tested.

Abstract

The modification of Nafion® membranes with polyaniline (PAni) has been studied as an alternative for reducing methanol crossover in direct methanol fuel cells (DMFC). The modification has been performed by directly polymerizing the PAni following two different routes: immersion (Naf-S-Y, where S mean surface and Y the number of hours exposition) and crossover (Naf-C-Y, where C means crossover). The former consist of exposing the membranes to a reactive solution containing the aniline, oxidant and catalyst; while in the latter the aniline and a solution with the oxidant and the catalyst are in different chambers separated by the membrane, thus forcing them to react inside

it. The effect of the modification mechanism and the reaction times has been studied. The resulting membranes were extensively characterized by means of Fourier Transform Infrared (FTIR), ionic exchange capacity (IEC), water uptake (WU), methanol permeability and single direct methanol fuel cell performance. Chemical characterization revealed that the oxidation state of the polyaniline was in all cases emeraldine and the amount of PAni for an equivalent exposure time was bigger for the crossover route. The crossover route has proven to be more effective in decreasing the apparent methanol permeability of Nafion modified membranes up to 48% for the crossover sample with higher modification time when the polymerization is due inside the membrane such is the case of the composite Naf-C-Y membranes. The Direct Methanol Fuel Cells performances of membrane-electrode assemblies prepared with pristine Nafion® and Nafion-PAni membranes were tested at 40, 60 and 80ºC under 2M methanol concentration. The results are compared to those found for Nafion® pristine membranes which power densities were 90, 65, 60 and 50 mW/cm^2 at 80ºC for Nafion®, Naf-S-1, Naf-S-5 and Naf-C-2, membranes respectively.

Key words: Characterization; Direct Methanol Fuel cells (DMFC); Polymer membranes; Fuel Cell; Polymer Membrane Fuel Cell (PMFC); Nafion/PAni membranes, methanol permeability, Membranes conductivity.

Introduction

Direct methanol fuel cells (DMFCs) are under attention as promising portable power generators for different electronic applications, e.g. telecommunication, military, leisure, etc[1]. As main advantages, DMFCs present ten to fifteen times more energy capacity than proton exchange membrane fuel cells (PEMFCs) and using hydrogen as feed and Li-batteries due to the liquid nature of the methanol and easy refueling [1-3]. However, one of the main challenges with DMFC is to reduce the high methanol permeability through the polymeric membranes used, such as pristine Nafion®, which lowers the DMFC performance due to fuel crossover [4,5].

With the incorporation of inorganic fillers such as sepiolite and silica gel into the matrix of Nafion, the methanol uptake for DMFCs can be reduced with respect to unmodified Nafion®[6-.11]. Sorption studies showed that the Nafion/silica and Nafion/sepiolite membranes had a larger affinity for water over methanol, whereas the order is reversed for pristine Nafion® membranes. Consequently, these experimental results suggest that the methanol permeability through the hybrid membranes will be lower that unmodified Nafion®[13,14]. It has also been suggested that nanofibers reinforced Nafion® membranes could be an interesting strategy to improve the DMFCs performance, while reducing the amount of Nafion® required, thus lowering the costs of the membrane preserving high performances. Using, for instance, PVA nanofibers for efficient solid electrolytes separation of the anode and the cathode together with the development of cheaper catalyst for fuel cell oxidation could lead to the development of commercial DMFC at low temperatures[15,16].

Recently, research interest has been focused on modified Nafion® membranes in electrode structures of fuel cells by conducting polymers such as polyaniline (PAni). Such studies show that the proton conductivity of the composite Nafion®/PAni

membranes is higher than Nafion® membranes at low humidity, due to the existence of the conjugated bonds in polyaniline that facilitate proton transfer and electronic conductivity at the PEM interface[17,18]. Indeed, protonated polyaniline directly polymerized on Nafion® 117 forming a composite membrane, produced a methanol blocking layer that reduced the methanol crossover in the direct methanol fuel cell (DMFC) by 59%, allowing beneficial operating conditions at high methanol concentration on a single fuel cell[19].

In earlier studies, we prepared and characterized composite Nafion® based membranes with PAni and investigated their morphology, conductivity, permselectivity and electrotransport phenomena [20-22]. The results of these studies pointed out those composite membranes had interesting properties as solid electrolytes for fuel cell applications for PEMFC of H_2/O_2. Consequently, we wondered if intercalation of the emeraldine form of polyaniline in the membrane via *in situ* polymerization would have a synergic effect on the DMFCs cells, by reducing methanol crossover and increasing the fuel cell performance.

In this work, the aniline polymerization process to modify the Nafion® membrane has been carried out following two different routes, named "immersion" and "crossover". The "immersion" modification is expected to develop a very thin layer of polyaniline on the Nafion® membrane surface. The effect of the PAni surface layer on the membrane should avoid the fuel cross through the membrane as well as to increase the overall corrosion resistance. Moreover, due to the proton conductivity of the polyaniline, the new modified membrane should improve the movement of the H^+ through the membrane. The "crossover" modification, which introduces the PAni inside the Nafion membrane, is expected to partially fill-in the internal spherical ionic clusters and thus prevent fuel crossover across the membrane, if we consider the ionic cluster model[23].

However, we can predict that too much PAni inside the membrane would lead to an excessive reduction on the membrane exchange capacity or even create a short-circuit in the membrane.

This work is aimed to investigate novel composite membranes, produced by polyaniline polymerization on a Nafion® membrane by "immersion" and "crossover" routes. Characterization of such membranes will be emphasized in chemical composition as well as in the variations of methanol flux and permeability, transport properties and electrochemical performance in DMFC applications.

Experimental Section

Materials and Chemicals

HNO_3 (60% wt), H_2SO_4 (96% wt), NaCl, $FeCl_3$, methanol (99.9%) and aniline (99%) were purchased from Sigma Aldrich and were used as received. Nafion® membrane was purchased from DuPont.

Membrane preparation

Nafion® composite membranes were prepared by polymerization of aniline in presence of Nafion® films. Before aniline polymerization, the Nafion® membranes were pre-treated by oxidative-thermal conditions[22], with the aim of converting them into their H^+ form and oxidizing the remaining products in the ionic clusters and channels. The membranes were sequentially boiled: first in 5% vol. HNO_3, then in 10% vol. H_2O_2, and finally in distilled water. In each solution the boiling lasted for 3 h.

Two different routes were studied, namely: immersion modification and crossover modification. The membranes obtained by immersion modification were prepared

according to the procedure suggested by Munar et al [22], schematized in Figure 1. The aniline polymerization was carried out in two steps at room temperature. The first step consisted of saturating the membranes in a solution of 0.01 M aniline + 0.5 M H_2SO_4 for 60 h in static conditions. Then, the samples were washed with water and placed in a triple solution of 0.01 M aniline, 0.01 M $FeCl_3$ in 0.5 M H_2SO_4 for different exposure times (without stirring). This method allows the modification of both membrane faces. The polymerization exposure times (second step) were 1, 2 and 5 hours. The membranes prepared were identified with the following code: Naf-S-Y, where S stands for surface modification and Y is the polymerization time, in hours.

The crossover modification procedure suggested in this work is based in the one proposed by Munar et al[22]. The aim of this procedure is to polymerize the aniline inside the membrane and not on the surface. To achieve this goal, the membrane is vertically fixed in the middle of a two-chamber cell: aniline is in one cell and the other polymerization reagents (oxidizing and catalyst) are in the other one. This set-up is schematized in Figure 2.

To polymerize the aniline inside the membrane the concentration of the oxidant (sulfuric acid) should be reduced and the concentration of aniline increased with respect to the conditions of the immersion modification method described previously[24]. Therefore, in cell A (Figure 2) it was introduced a solution of 0.01 M $FeCl_3$ in 0.1 M H_2SO_4 and in cell B an aniline solution of 0.3M.

Two different exposure times were used: 2 and 4 hours. During this time, both chamber-cells were kept under continuous stirring. Then, the samples were washed with water. The membranes prepared were identified with the following code: Naf-C-Y, where C stands for crossover modification and Y is the polymerization time, in hours.

Chemical characterization

The chemical and thermal properties of the membranes were characterized using the following techniques: elemental analysis, Fourier-transformed infrared spectroscopy (FTIR) and thermogravimetric analysis (TGA).

For all instrumental techniques, membranes were conditioned in 0.5M H_2SO_4 for 2 hour at room temperature. Then, the membranes were dried under vacuum at 80ºC for at least 20h before testing.

The **elemental composition** of the samples (C, S, N) was determined using a sulfur and carbon elemental analyzer Leco SC-144DR and a nitrogen analyzer Leco FP-528.

The Fourrier-transformed infrared **(FTIR)** spectra were recorded using a JASCO model FT/IR-6200 at room temperature in attenuated total reflection (ATR) mode with a diamond/ZnSe crystal. 32 scans were collected in the range of 600-4000 cm-1 wave numbers with a spectral resolution of 4 cm^{-1}. A background scan of clean diamond/ZnSe crystal was acquired before scanning the samples.

The **TGA** thermograms were recorded using a TG-STDA Mettler Toledo model 851e /LF/ 1600 at a heating rate of 10ºC/min from 50 to 900ºC under N_2 atmosphere using a flux of 60 ml/min.

Transport properties characterization

The membrane transport properties were assessed by ionic-exchange capacity, water uptake and methanol permeability. To evaluate the ion-exchange capacity (**IEC),** all membranes were set in their acid form, i.e. protonated, by placing them in 1 M H_2SO_4 for 24 hours. Then, they were washed by immersion in water for 30 min and rinsed before being dried under vacuum at 80ºC for at least 20h. Afterwards, the membranes were immersed in 1 M NaCl solution for 24h to exchange protons with sodium ions.

Once the membranes were protonated, the IEC value was determined by titration of the released amount of protons with a 10^{-2} M NaOH solution and using phenolphthalein as indicator.

To determine the water uptake (**WU**) the membranes were previously set in their acid form. After washing and rinsing, the membranes were immersed in water at room temperature for 24h. Then, the water-swollen membranes were taken out, blot dried with filter paper and weighed immediately. Finally, the membranes were dried under vacuum at 80ºC for at least 20 h and weighed again. This operation was repeated three times. Water uptake was obtained as follows:

$$WU(\%) = \frac{w_w - w_d}{w_d} x100 \quad (1)$$

Where w_w and w_d are the weight of the wet and dry membrane, respectively.

The methanol permeability coefficient through the composite membranes was measured following the procedure reviewed by Mollá and Compañ[25], using a two-identical-compartment glass cell. The membrane was placed between both compartments, where Chamber A was filled with a 2 M methanol solution and chamber B was filled with water. Both compartments were stirred and thermostatized at 20 and 70 ºC, respectively, during the permeation experiments.

The concentration of methanol in compartment B was measured as a function of time using a gas chromatograph (GC, Varian model 3900) with a capillary column (BP20 - SGE- length 30m, I.D. 0.25mm, film 0.25µm, P/N).

The diffusion process of methanol across the membrane in the stationary state is described by the Fick's law by mean of the expression

$$j = \frac{dn}{A \cdot dt} = P \frac{(C_A - C_B)}{L} \quad (2)$$

Where, *j* represent the flux density of methanol, *n* is the amount of methanol crossing the membrane expressed in moles, *A* is the area, *t* the time, *P* is the apparent methanol permeability coefficient, C_A and C_B the methanol concentration in chambers A and B, respectively, and *L* the thickness of the membrane.

The apparent methanol permeability coefficient (*P*) can be determined following the procedure described by Mollà and Compañ[25] from the slope of the methanol concentration in chamber B (C_B) vs. diffusion time (t) plot, since they are related as follows:

$$C_B(t) = \frac{P \cdot A \cdot C_A}{V_B \cdot L}(t - t_0) \quad (3)$$

where V_B is the volume of liquid in compartment B and t_0 the time lag.

Fuel cell performance

Preparation of membrane electrode assembly (MEA)

Prior the MEAs preparation and membrane performance determination in the single fuel cell system, the membrane was activated following the following procedure: 1) the membrane was boiled during 1 hour in distilled water. 2) After this, the membrane was immersed during 1 hour in a solution of sulfuric acid at 80ºC and, 3) the membrane was introduced during 1 hour in distilled water at 80ºC. Subsequently, membrane electrode assemblies (MEAs) were prepared with such membranes to study their DMFC performance. The MEAs were arranged by sandwiching the membrane between two gas diffusion layers (GDL) which were further hot pressed at 120ºC and 3.5 bar for 5 min.

The MEAs prepared were tested in the single cell hardware described previously[15]. The anode and cathode were acquired from BalticFuelCells GmbH (Schwerin, Germany). The anode is composed of a carbon paper gas diffusion layer (GDL) from

Freudenberg&Co (Weinheim, Germany), model H2315 T105A, covered by an alloy of Pt-Ru black 50:50 (Alfa Aesar) with a catalyst loading of 5.0 mg cm^{-2} together with a 20wt% of dry Nafion® ionomer. Similarly, the cathode was composed of a GDL from Freudenberg, model H2315 I3C4, with a catalyst loading of 5.0 mg cm^{-2} of Pt, containing platinum nanoparticles (≈ 5 nm size) supported by advanced carbon (HiSPEC 13100, Alfa Aesar) with a Pt/C ratio of 70% (weight) and a 20 wt% of dry Nafion® ionomer. For comparison purposes, measurements were also carried out with commercial Nafion® 115 membranes (DuPont Co.).

The MEAs, previously equilibrated with water, were placed into a square 5 cm^2 active area fuel cell hardware (quickCONNECT, BalticFuelCells GmbH) containing graphite serpentine flow fields and equipped with a pressure-controlled clamping force system. This latter characteristic enables to exert a constant contact resistance between membrane and electrodes.

Fully hydrated conditions were assured in the anode side of the cell, flooded with deionized water to prevent dryness of the membrane. A 2 M methanol solution in water pumped at a flow rate of 5 ml/min was used to feed the anode, whereas high purity oxygen (99.99%) was introduced to the cathode with a flow rate of 150 ml/min and at atmospheric pressure. No gases were flowing across anode and cathode during the experiments.

Single fuel cell performance

MEAs were activated for 5-6 hours by alternating different current demands until a stable operation was achieved. This procedure helps to open new pores and channels into the catalytic layers so more fuel and oxygen can reach the catalyst particles and enhance performance of the electrodes. Then, current density vs. potential (I-V) curves

were obtained at 40ºC, 60ºC and 80ºC from open circuit voltage (V_{OC}) conditions up to 0.2 Volts by manual stepwise increment of the current density and waiting for 2 minutes in each measurement, assuring the reading of a voltage near a steady-state value. Power density values were then calculated and plotted.

Results and Discussion

Chemical and structural characterization

In both immersion and crossover methods, there is a significant color change in the membranes according to the type and time of modification performed. As the polymerization time increases the membrane turns blue and rapidly evolves to emerald-green. The transparent Nafion® membrane, in its original conditions, gets a soft green color at low reaction times, becoming more intense and dark with increasing polymerization time. The color variation is believed to be due to the polymerization of aniline, in the form of emeraldine[20,21]. The green "emerald" emeraldine, indeed, is the only oxidation state of polyaniline that allows electron conductivity. Therefore, it is possible to confirm the polymerization of aniline in emeraldine form at unaided eye. This hypothesis is proved in a later section by Fourier transform infrared spectroscopy (FTIR). The increase on green intensity of the samples with exposure time corresponds with an increase in the amount of polymerized aniline.

Elemental analysis

Elemental analysis was performed to determine the content of the main chemical elements present in the samples (carbon, sulfur and nitrogen). The resulting elemental composition for Nafion® and Nafion®- modified membranes is summarized in Table 1.

The detection of nitrogen in the modified membranes confirms the presence of polyaniline, being their concentrations proportional to the amount of polyaniline

polymerized in the sample. In order to estimate the exact content of PAni polymerized in the membranes, the following relationship has been used:

$$\%PANI = \frac{\frac{\%N}{\%N_{PANI}}}{\frac{\%N}{\%N_{PANI}} + \frac{\%S}{\%S_{Nafion}}} x100 \quad (4)$$

Where N_{PAni} is the weight fraction of nitrogen in the emeraldine form of polyaniline, S_{Nafion} is the weight fraction of sulfur in Nafion® membranes (data obtained from elemental analysis) and %N and %S are the nitrogen and sulfur percentages of the samples as determined by elemental analysis. Table 1 shows the variation of polymerized aniline (%PAni) of Nafion®-modified membranes with increasing aniline polymerization times using both immersion and crossover routes.

The rate of polyaniline incorporation to the membranes by the immersion route is significantly less than in the case of the crossover route. This is best shown comparing the %PAni values obtained for samples Naf-S-5 and Naf-C-2, where they both show similar values but the exposure time in the case of the crossover sample is 40% less. In any case, the results support the aforementioned hypothesis: increasing polymerization times show an increase in the intensity of the green color of the resulting membranes due to higher PAni content.

Fourier Transform Infrared FTIR-ATR Spectroscopy

Figure 3 shows the FTIR-ATR spectrum of Nafion® and Nafion®/PAni membranes ranging from 4000 to 600cm^{-1}, confirming the presence of PAni. In Figure 3.b it can be better seen the FTIR spectra of the samples in the range from 2000 and 1400 cm^{-1}, where the bands at 1570cm^{-1} and 1473cm^{-1} stand clearly, being attributed to the quinoid and benzenoid stretching modes of the polyaniline, respectively [24-27]. The C-H

stretching within the region 3200-2800 cm^{-1} is weak, indicating saturated benzene rings[28].

Other important difference seen in FTIR spectra is the intensity reduction of the band associated with the H_3O^+ species at around 1710 cm^{-1} in the case of Nafion®-modified membranes. This suggests that the Nafion®-modified membranes are less hydrophilic than Nafion®, given that all membranes were dried under the same conditions, similarly as observed by Tan et al.[24]

Thermogravimetric Analysis (TG-DTG)

The thermal stability of the Nafion® and Nafion®-modified membranes was studied by TGA under air atmosphere. For the sake of clarity, Figure 4 illustrates TGA and differential thermogravimetric (DTG) curves of Nafion® and Nafion®-modified membranes with the highest PAni content for each modification method (i.e. Naf-S-5 and Naf-C-4).

The Nafion® DTG curve (Figure 4.b) exhibits transitions at the temperature ranges of 25-290°C, 290-390°C, 390-470°C, and 470-520°C. According to the literature for Nafion® membranes, the phenomena that can occur associated to these transitions is[29]:

i) Gradual loss of water from 25 to 290 °C.

ii) Desulfonation (with the loss of SO_2) combined with the decomposition of the ether groups (C-O-C) on the side-chains, between 290 and 400 °C.

iii) Side-chain decomposition at 400 to 470 °C

iv) Decomposition of the poly(tetrafluoroethylene) backbone at 470 to 560 °C.

Nafion® modified membranes show five transitions, referred as i' to iv' in both Figure 4.a and Figure 4b. The first four stages are in concordance with the four decomposition stages given above for Nafion® (i-iv). The fifth transition (v') is related to combustion of the graphite products derived from the degradation of polyaniline[30-33].

The mass loss due to water in both Nafion® modified membranes is slightly lower than in the case of the neat Nafion® membrane. This fact can be related with the lower hydrophilicity of the membranes, already observed by FTIR spectra, after the modification with PAni[34].

DTG curves of Nafion®-modified membranes indicate that the degradation of the sulfonate groups starts at a lower temperature than unmodified Nafion®. Indeed, the sharpness of the DTG peak at 330-350ºC in Figure 4.b points out that desulfonation occurs faster with the presence of PAni in the membrane. This results can be explained if we assume that the aniline was primarily polymerized in the ionic cluster regions of Nafion®, acting as a catalyst for enhanced removal of the sulfonate groups above 300ºC, as suggested by Tan et al. and Yang et al.[24,35]. However, this could only be possible if there is a high molecular contact between the sulfonate groups and the PAni surface. Therefore, TGA would be indicating that PAni polymerization takes place inside the ionic cluster regions of Nafion® in both modification methods.

Figure 4 also reveals a delay in the decomposition temperature of the poly(tetrafluoroethylene) backbone in Nafion®-modified membranes (iv') regarding to the Nafion® ones (iv). Such delay is attributed to the generation of a protective layer from the degradation products of PAni. This layer hampers the volatilization of degradation products released in the decomposition of the main structure of Nafion®. It can be highlighted that this phenomenon occurs to a greater extent in the membranes obtained by crossover, rather than in membranes produced by immersion route.

Transport properties characterization

Water uptake and Ionic-exchange capacity (IEC)

The membranes water uptake is summarized in Table 2. Lower values of water uptake were found in all the modified samples. This trend is more pronounced as the PAni content is higher, in agreement with FTIR and TGA observations. Hence, the polymerization of PAni in the percolation channels of the Nafion® leads to a lower hygroscopicity of the membranes as a consequence of a minor free volume inside them.

At this point, it could be supposed that polymerization of the PAni inside the Nafion® membrane could have collapsed the percolation channels of the membrane. Analyzing the IEC of the modified membranes, also shown in Table 2, showing a minor decrease (<4%) in its value for all modified membranes, it can be deduced that percolation channels of the modified samples are still open and accessible. Nevertheless, it can be noticed that crossover samples show lower IEC values than immersion ones, as well as IEC decreases with increasing polymerization time.

Methanol permeability

The methanol transport across Nafion®-modified membranes was characterized according to the procedure and calculations described by Mollà et. al.[25].The methanol permeability was assessed at two different temperatures, at room temperature and 70°C, close to the operating conditions of the DMFC.

Figure 5 plots the minimum square correlation slopes obtained at room temperature and at 70°C for Nafion® membranes as well as all the Nafion®/PAni ones. Putting this data into equation (3) allows assessing apparent methanol permeability of the membranes (P). Table 3 collects the apparent permeability coefficients obtained for all the membranes and their permeability variation with respect to Nafion® membranes.

It can be deduced from those results that modification of the membrane by the immersion route did not produced a reduction in methanol membrane permeability. Moreover, at room temperature as well as at 70ºC, the apparent methanol permeability coefficients for samples modified by immersion are higher than those of unmodified Nafion® membranes. Therefore, it can be concluded that the immersion route does not improve barrier properties to methanol. Nevertheless, within these samples, the longer the polymerization time, the better the barrier performance.

On the other hand, the modification of membranes by crossover route decreases the apparent methanol permeability coefficients, partially blocking methanol transport across the membranes. At room temperature, the Naf-C-2 sample shows a decreasing of 22% in methanol permeability and 48% in the case of Naf-C-4. Likewise, Nafion®/PAni samples at 70 °C show a similar trend, indicating a link between the reduction of membrane permeability and the polimerization time of the membranes in the crossover modification route. This can be explained considering that the aniline polymerization has taken place inside the ionic cluster regions of Nafion®, as described by Munar et al[22] and in agreement with the previous analysis, reducing the methanol crossover through the membrane.

Fuel cell performance

Membrane electrode assemblies (MEAs) were prepared using the Naf-S-1, Naf-S-2, Naf-S-5, Naf-C-2 and Naf-C-4 membranes to study their DMFC performance. Also for comparison purposes, MEAs with Nafion®-112 were tested using identical conditions than the composite membranes. Figure 6 shows the polarization curves (cell potential, V, and power density, P, versus current density, *i*) for the MEAs prepared when DMFC were operated at 40, 60 and 80ºC of temperature.

The maximum power density for the MEA of Nafion-PAni membrane was about 50, 60, 62 and 87 mW/cm^2 at 80ºC, for Naf-C-2, Naf-S-1, Naf-S-5 and pristine Nafion® , respectively. We think that this result can be related with the increasing of the ohmic resistance as a consequence of the aniline concentration increase, being the crossover route the one that causes higher power loss, such as is shown in figure 6. While in the literature one can find several papers reporting the performance of pristine Nafion®, composites of Nafion® and impregnated membranes, the results cannot always be easily compared with each other since the experimental conditions differ.

A close inspection on the I-V curves in Figure 6 shows two different regions: Region-I, in which the activation process of the MEA occurs, controlled by low current densities; and region-II, typically at current densities *i* above 200 mA/cm^2, which is characterized by showing a linear behavior with a negative slope. The latter region is dominated by the protonic resistance of the membrane and just slightly by methanol crossover, which can be attributed to mechanisms of diffusion and electro-osmosis[36-38].

The cell voltage of a DMFC can be written as[39]

$$V = V_{OC} - A_1 \ln \frac{i}{i_0} - i \cdot R \cdot S - \eta_{cros} \quad (5)$$

where V is the cell voltage, V_{OC} the reversible open circuit voltage, i the current density, i_0 the current density at which the over-voltage begins to move from zero, A_1 the sum of the slopes of the polarization curves for anode and cathode, R is the ohmic resistance of the MEA, S is the area of the assembly membrane-electrodes exposed to the methanol flux and η_{cros} is the overpotential produced by methanol crossover.

The cell voltage of the MEAs prepared with our membranes can be modeled by means of equation (6) as reported by several authors[40-42]

$$V = V_{OC} - A_1 \ln \frac{i}{i_0} - i \cdot R \cdot S - m \exp(n \cdot i) \quad (6)$$

where m and n are empirical parameters associated with mass transport limitation phenomena.

We have fitted the experimental data of the polarization curves with a model based on this latter equation, thus obtaining the parameters A_1, i_0, R, m and n, while keeping the values measured for open circuit voltage, V_{OC}.

Figure 7 shows the fitting between some experimental and modelled curves for Nafion® and Nafion® modified membranes, where it can be observed that the eq. (6) fits very well with the results of performance obtained at T=80ºC. Similar fit results were obtained for the other temperatures. The values obtained for the fit parameters from all curves shown in Fig. 6 are summarized in Table 4.

The V_{OC} values obtained from polarization curves can be used indirectly asses the fuel cell performance. It can be seen in Table 4 that V_{OC} values increase in all cases with the temperature, favoured by the accelerated electrochemical reactions. However, V_{OC} does not reach the theoretical value at the given temperature, being such reduction attributed to the catalyst efficiency and methanol crossover by diffusion[39]. In this sense, it is worth to remark that the V_{OC} value of the Nafion®-modified membrane Naf-C-2 under real DMFC operation (80ºC) is the highest. This could be related with the fact that this Nafion/PAni membrane showed the lowest methanol permeability and therefore, lower methanol crossover and cathode losses caused by the methanol. Regarding the variations depending on the membrane modification, a similar trend can be found for all temperatures, where V_{OC} (Naf-C-2) > V_{OC} (Naf-S-5). In agreement with the methanol permeability values shown in Table 3. However, it must be kept in mind, not only the methanol crossover is known as responsible on the V_{OC} parameter, another factors as

electrodes catalyst loading, MEA preparation, water management and blocking of pores in GDL, proton conductivity, catalytic activity and reaction kinetics, concentration methanol as fed, pressure and temperature, air/oxygen gas flow on the cathode, etc., can have influence on V_{OC} values. Unfortunately, all these parameters are difficult to control together.

As usual, the open circuit voltage V_{OC} sharply decreases from the thermodynamic electromotive force of the cell to a value in the vicinity of 0.6 for Nafion® and Naf-S-Y membranes and up to 0.67 V in case of Naf-C-2 membranes. This sharp decrease is caused by internal currents, activation energy and, specially, by fuel crossover[39].

Looking at the resistance of the membranes at 80ºC in Table 4, which were obtained from the V-I curves linear behavior at i >150mA/cm^2, we find values ranging between 0.13Ω for pristine Nafion® and 0.23Ω for Naf-C-2. These values affect the performance of the cells, as it can be observed in the maximum power density obtained in polarization curves of Fig. 6. The values of the ohmic resistance obtained from the polarization curves are in fair agreement with those measured directly by impedance spectroscopy in the MEAs built with the same membranes.

For each membrane, the parameters i_0 and A_1 also show a decrease as the temperature increases (see table 4). Since both parameters are related with the catalytic activity of the catalyst layer at the electrodes, this would suggest that as the methanol crossover rises with the temperature, the specific active area of the catalyst should diminish as a consequence of the undesired reaction between the methanol and the oxygen.

The overpotential due to the methanol crossover, η_{cros}, can be calculated following the procedure described by Li-Ning Huang et al.[43] and S. Mollá and V. Compañ [44] by mean of the expression:

$$\eta_{cros} = \chi J_{MeOH} = \chi(J_{con} + i \cdot J_{cros}) \tag{7}$$

where χ is a constant and J_{MeOH} the flux of methanol crossing the membrane. Assuming that this flux (J_{MeOH}) has a current independent term affected by methanol concentration C_{an} at anode, i.e. J_{con}, and a current dependent term due to electro-osmosis of methanol, i.e. J_{cros}. In our study we suppose that J_{con} is a Fickean diffusion flux with linear concentration gradient dependence across the thickness of the membrane, i.e. diffusion coefficient is independent of the concentration differential between anode and cathode sides, and the methanol molecules penetrating from anode and cathode are catalytically oxidized. Thus, J_{con} becomes a dependent term of the methanol concentration in anode,

$$J_{con} = k \cdot C_{an} \tag{8}$$

being k a constant which depends on the methanol diffusivity across the membrane. By substituting eq.8 into eq.7, rearranging eq.6 and separating the C_{an}-dependent and i-dependent terms, it results the following expression:

$$V(i, C_{an}) = V_{OC} - A_1 \ln\left(\frac{i}{i_0}\right) - A_2 \cdot C_{an} - A_3 \cdot i \tag{9}$$

with

$$A_2 = \chi \cdot k \tag{10}$$

$$A_3 = R \cdot S + \chi \cdot J_{eos} \tag{11}$$

where A_2 is a term relating the overvoltage to the methanol crossover by diffusion and A_3 is a term relating the overvoltage influenced by the sum of the protonic resistance

and the methanol electro-osmotic effects. These equations are only valid in the region-II of the polarization curves (Voltage vs current density). The derivative $\frac{dV}{di}$ when the concentration of the methanol in the anode is constant, is equal to,

$$\frac{dV}{di} = -\frac{A_1}{i} - A_3 \tag{12}$$

At current densities above 150 mA/cm^2, $\frac{A_1}{i} < \frac{A_1}{100} << A_3$. Then we can suppose negligible the first term in equation (11), and then, A_3 can be obtained from the slope of the plot of *V* vs. *i* at a fixed temperature as well as methanol feed concentration C_{an} and *i* >150 mA/cm^2. Figure 8 shows the variation of the cell voltage, V, versus *i* for MEAs prepared with Nafion® and Nafion/PAni membranes in the region between 100 mA/cm^2 and 300 mA/cm^2 where the methanol crossover can be attributed to mechanisms of diffusion and electro-osmosis.

Similarly, following the procedure described above from eq.(12) we have obtained the parameter A_3 and from their estimation together with eq (11), in order to calculate the values of $\chi \cdot J_{eos}$. Since A_3 relates the overvoltage to a combination of protonic resistance, i.e. $R_{\cdot}S$, and methanol crossover by electro-osmosis, i.e. $\chi \cdot J_{eos}$, this latter parameter can be estimated by subtracting the term $R_{\cdot}S$ from A_3. The values calculated for the neat Nafion® and Nafion/PAni membranes at different temperatures, are given in Table 5.

The parameter A_3, which is related to the ohmic resistance of the membrane, decreases in each membrane as the temperature increases, due to the activation phenomenon of the proton conductivity. This results shows that the parameters $\chi \cdot J_{eos}$ are practically the same at all temperatures for Nafion® and Naf-S-1 membranes, decreasesing when the

temperature increase. Nafion® modified membranes S-5 and C-2 show and increase of 20 and 50% respectively, with respect to pristine Nafion® membrane at all temperatures. This behavior can be due to the higher amount of protons transported by diffusion as H_3O^+ ion with relation to those transported by the Grottus mechanism. Similar results have reported by Luo et al.[45], where that electro-osmotic drag coefficient of water in Nafion® membrane rises with increasing temperature.

This results are related with the values of methanol flux, calculated using the equation (3), which are in $mol \cdot cm^{-2} \cdot s^{-1}$, 0,45x10-6, 3,0x10-6, 2,79x10-6 for Naf-S-1, Naf-S-5, Naf-C-2 respectively, and 3.63x10-6 for Nafion® membranes, at 70ºC of temperature, while the values at 30ºC are 1,41x10-6, 0,97x10-6, 0,72x10-6for Naf-S-1, Naf-S-5, Naf-C-2 respectively, and 0,92x10-6 for Nafion® membranes in the same units than above. The increase in PAni (from S-2 to S-5 or C-2) reduces the methanol flux, as could be expected. However, the variation with respect to pristine membrane is rare. Since there is no apparent reason to justify the increase of crossover for the surface modifed Nafion® membranes, we thing that some heterogeneities in the surface or in the thickness of the membranes during the PAni deposition process could be responsible for such variations.

Conclusions

Two different in situ polymerization methods were used to modify Nafion® membranes with polyaniline in the emmeraldine form. The modified membranes were extensively characterized, showing clear difference in the result depending on the polymerization method. Hence, the crossover route leaded to a modification inside the membrane, while the immersion route modification resulted in a more superficial growth of the PAni. In

both cases, the PAni polymerization has taken place in the ionic clusters, as derived from the morphological and thermal characterization. A decrease in the water sorption capacity has been found in the modified membranes when compared with neat Nafion®, being proportional to the amount of PAni in the membrane, however, no significant obstruction of the percolation channels has been caused, as derived from the IEC determinations.

The results of permeability tests of the membranes modified by the so-called crossover route show a improvement in methanol crossover resistance through the membrane. This behavior is considered to be due to polymerization of aniline inside the ionic domains of Nafion®.

The DMFC performances of membrane-electrode assemblies prepared with the Nafion-PAni membranes tested at 40, 60 and 80ºC under 2M methanol concentration have a behavior related with the ohmic resistance and methanol electroosmotic flux. PAni modification increases both parameters, being the crossover route (Naf-C-2) more influence than surface deposition (Naf-S-5). The values of power densities found for Nafion® and Nafion/PAni membranes were 90, 65, 60 and 50 mW/cm^2 at 80ºC for Nafion®, Naf-S-1, Naf-S-5 and Naf-C-2, membranes respectively.

Acknowledgments

This research is in the frame of Support Program for Research and Development of the Polytechnic University of Valencia and the Ministry of Science and Innovation for funding provided through the projects: SP-ENE-20120718 and 24761, respectively.

References

1. A. Carbone, R. Pedicini, G. Portale, A. Longo, L. D'Ilario, E. Passalacqua. J. Power Sources 163 (2006) 18–26.

2. S.K. Kamarudin, F. Achmad, W.R.W. Daud, Overview on the application of direct methanol fuel cell (DMFC) for portable electronic devices, International Journal of Hydrogen Energy 34 (2009) 6902-6916.

3. V. Neburchilov, J. Martin, H. Wang, J. Zhang. Journal of Power Sources 169 (2007) 221-238.

4. J. Muller, G. Frank, K. Colbow, D. Wilkinson, in: W. Vielstich, A. Lamm, H.A. Gasteig (Eds), Handbook of Fuel Cells-FFundamentals Technology and Applications, vol. 4, Jhon Wiley& Sons Ltd., 2003 (Chapter 62).

5. M. Neergat , K.A. Friedich, U. Stimming, in: W. Vielstich, A. Lamm, H.A. Gasteiger (Eds), Handbook of Fuel Cells-FFundamentals Technology and Applications, vol. 4, Jhon Wiley& Sons Ltd., 2003 (Chapter 63).

6. F.J. Fernandez-Carretero, K. Suarez, O. Solorza, E. Riande, V. Compañ. Journal of New Materials for Electrochemical Systems 13, (2010) 191-199.

7. F.J. Fernandez-Carretero, V. Compañ, E. Riande, J. Power Sources 17, (2007) 68-76.

8. A. Saca, A. Carbone, E. Passalacqua, A. D'Epifanio, E. Traversa, E. Sala, F. Traini, R. Ornelas, J. Power Souces 152 (1) 2005) 16-21.

9. R.A. Zoppi, et al… Polymer, 39 (1998) 1309-1315.

10. K.A. Mauritz. Mat. SSci. Eng., C-Biomimetic-Supramoleculkar Syst. 6 (2-3) (1998) 121-133.

11. P Staiti, A.S. Arico, et al.. Solid State Ionics 145 (2001) 101-107.

12. Christian Beauger, Guillaume Lainé, Alain Burr, Aurélie Taguet, Belkacem Otazaghine. J. Membr. Sci. 430 (2013) 167-179.

13. N. Miyake et al. J. Electrochem. Soc. 148(8) (2001)A905-A909.

14. Z.G. Shao, X, Wang, I.M. Hsing. J. Membr. Sci. 210 (2002) 147.

15. S. Moya, V. Compañ. Polyvinyl alcohol nanofiber reinforced Nafion membranes for fuel cell applications. J. Membr. Sci. 372 (2011) 191-200.

16. S. Molla, V. Compañ. J.Power Sources. 196 (2011) 2699-2708.

17. H. Gharibi, M Zhiani, R.A. Mirzaie, M. Kheirmand, A.A. Entezami, K.Kakaei, M. Javaheri, J. Power Sources 157 (2006) 703.

18. Jinyan Yang, Pei Kang Shen, John Varcoe, Zidong Wei, J. Power Sources, 189 (2009) 1016.

19. C.H. Wang, C.C. Chen, H.C. Hsu, H. Y. Du, C.P. Chen, J.H. Hwang, L.C. Chen, H.C. Shiuh, J. Stejskal, K.H. Chen. J. Power Sources 190 (2009) 279.

20. V. Compañ, E. Riande, F.J. Fernandez-Carretero, N.P. Berezina, A.A.-R Sytcheva, J. Membr. Sci, 318 (2008) 255.

21. N.P. Berezina,, N.A. Kononenko, A.A.-R Sytcheva, N.V. Loza, S.A. Shkierskaya. N. Hegman, A. Pungor, Electrochim. Acta 54 (2009) 2342

22. A. Munar, K. Suarez, O.Solorza, N.P. Berezina, V. Compañ, JES 157 (2010) B1186-B1194.

23. Hsu, W.Y. and T.D. Gierke, *Ion transport and clustering in nafion perfluorinated membranes.* Journal of Membrane Science, 1983. 13(3): p. 307-326.

24. Tan, S. and D. Belanger, *Characterization and transport properties of Nafion/polyaniline composite membranes.* Journal of Physical Chemistry B, 2005. 109(49): p. 23480-23490.

25. Molla, S., Compañ, V; Lafuente S.L.; Prats, J., On the Methanol Permeability through Pristine Nafion (R) and Nafion/PVA Membranes Measured by Different Techniques. A Comparison of Methodologies. Fuel Cells, 2011. 11(6): p. 897-906.

26. Chiang, J.C. and A.G. Macdiarmid, *Polyaniline - Protonic Acid Doping of the Emeraldine Form to the Metallic Regime.* Synthetic Metals, 1986. 13(1-3): p. 193-205.

27. Trchova, M., et al., FTIR spectroscopic and conductivity study of the thermal degradation of polyaniline films. Polymer Degradation and Stability, 2004. 86(1): p. 179-185.

28. Prasad, K.R. and N. Munichandraiah, Potentiodynamic deposition of polyaniline on non-platinum metals and characterization. Synthetic Metals, 2001. 123(3): p. 459-468.

29. de Almeida, S.H. and Y. Kawano, *Thermal behavior of Nafion membranes.* Journal of Thermal Analysis and Calorimetry, 1999. 58(3): p. 569-577.

30. Avlyanov, Z.K., et al., *Study of Thermal-Stability of Polyaniline.* Vysokomolekulyarnye Soedineniya Seriya B, 1990. 32(10): p. 735-738.

31. Kulkarni, V.G., L.D. Campbell, and W.R. Mathew, *Thermal-Stability of Polyaniline.* Synthetic Metals, 1989. 30(3): p. 321-325.

32. Hagiwara, T., M. Yamaura, and K. Iwata, *Thermal-Stability of Polyaniline.* Synthetic Metals, 1988. **25**(3): p. 243-252.

33. Chandrakanthi, N. and M.A. Careem, *Thermal stability of polyaniline.* Polymer Bulletin, 2000. 44(1): p. 101-108.

34. Bong Gill Choi, HoSeok Park, Hun Suk Im, Yo Jin Kim, Won Hi Hong. Journal of Membrane Science 324 (2008) 102-110.

35. Yang, J.Y., Pei Kang Shen, John Varcoe, Zidong Wei. Journal of Power Sources, 2009. **189**(2): p. 1016-1019.

36. M. Hellen, B. Viswanathan, S. Srinivasa Murthy, J. Power Sources 163 (2006) 433-439.

37. G. Murgia, L. Pisani, A.K. Shukla and K. Scott, J. Electrochem. Soc. 150 (2003) A1231-A1245.

38. K. Scott, W. Taana, J. Cruickshank, J. Power Sources 65 (1997) 159-171.

39. J. Larminie, A. Dicks, Fuel Cell System Explained, John Wiley&Sons Ltd., Chichester, England, 2000 (Chapter 3).

40. J. Kim, S.M. Lee, S. Srinivasan, C.E.Chamberlin. Modeling of proton exchange membrane fuel cell performance with an empirical equation. J. Electrochem. Soc. 1995;142:2670-2674.

41. F. Laurencelle, R. Chahine, J. Hamelin, K. Agbossou, M. Fournier, T.K. Bose, A.Laperrière. Characterization of a Ballard MK5-E Proton Exchange Membrane Fuel Cell Stack. Fuel Cells 2001;1:66-71.

42. L. Pisani, G. Murgia, M. Valentini, B. D'Aguanno. A new semi-empirical approach to performance curves of polymer electrolyte fuel cells. J. Power Sources 2002;108:192-203.)

43. Li-Ning Huang, Li-Chun Chen, T. Leon Yu, Hsiu-Li Lin, J. Power Sources 161 (2006) 1096-1105.

44. S. Mollá, V. Compañ. J. Power Sources, 196 (2011) 2699-2708.

45. Z Luo, Z Chang, Y Zhang, Z Liu, J. Li. Int. J. Hydrogen Energy 35 (2010) 3120-3124.

TableS

Table 1. Elemental composition of Nafion and Nafion/PAni membranes.

Sample	% C	% S	% N	% PAni
Nafion	14.12	2.11	0.00	0
Naf-S-1	13.98	1.73	0.35	2.69
Naf-S-2	14.04	1.68	0.42	3.30
Naf-S-5	12.36	1.47	0.58	5.11
Naf-C-2	13.17	1.44	0.55	4.95
Naf-C-4	12.63	1.33	0.71	6.79

Table 2: Water uptake and EIC values of Nafion and all modified membranes.

Sample	Water uptake (% wt)	EIC (mmol/g)
Nafion	35.9±1.5	877.7
Naf-S-1	28.4±1.6	872.7
Naf-S-2	27.0±0.2	872.1
Naf-S-5	30.6±4.9	864.9
Naf-C-2	26.1±1.1	870.7
Naf-C-4	26.7±0.2	843.8

Table 3: Slope, apparent methanol permeability coefficient and variation permeability of Nafion and all modified membranes at room temperature and 70ºC

Sample	**Room temperature**			**Temperature = 70°C**		
	Slope (mol/(L·s))	P (cm^2/s)	Variation permeability (%)	Slope (mol/(L·s))	P (cm^2/s)	Variation permeability (%)
Nafion	$4{,}30 \cdot 10^{-6}$	$2{,}40 \cdot 10^{-6}$	-	$1{,}70 \cdot 10^{-5}$	$9{,}45 \cdot 10^{-6}$	-
Naf-S-1	$6{,}59 \cdot 10^{-6}$	$3{,}67 \cdot 10^{-6}$	+53	$2{,}11 \cdot 10^{-5}$	$1{,}17 \cdot 10^{-6}$	+24
Naf-S-2	$5{,}05 \cdot 10^{-6}$	$2{,}82 \cdot 10^{-6}$	+17	$1{,}71 \cdot 10^{-5}$	$9{,}52 \cdot 10^{-6}$	+1
Naf-S-5	$4{,}50 \cdot 10^{-6}$	$2{,}51 \cdot 10^{-6}$	+5	$1{,}42 \cdot 10^{-5}$	$7{,}91 \cdot 10^{-6}$	-16
Naf-C-2	$3{,}35 \cdot 10^{-6}$	$1{,}87 \cdot 10^{-6}$	-22	$1{,}30 \cdot 10^{-5}$	$7{,}25 \cdot 10^{-6}$	-23
Naf-C-4	$2{,}25 \cdot 10^{-6}$	$1{,}26 \cdot 10^{-6}$	-48	$1{,}01 \cdot 10^{-5}$	$5{,}65 \cdot 10^{-6}$	-40

Table 4. Summary of the parameters of Eq.(13) describing the polarization curves V *vs.* i for the MEAs prepared with Nafion 212, and Nafion-PAni composites prepared by immersion and crossover using different times of cross linking in a single Direct methanol fuel cell, (DMFC).

Membrane	**Temperature [°C]**	**Voc [V]**	**i_0 (mA/cm^2)**	**A_1 (V)**	**R (Ohm)**	**m (V)**	**n (cm^2/mA)**
Nafion212	40	0.566	60	0.039	0.157	2.5E-03	0.89
	60	0.601	25	0.017	0.140	2.0E-02	0.97
	80	0.629	20	0.017	0.132	2.2E-02	0.45
Naf-S-1	40	0.561	51	0.035	0.163	1.3E-02	1.0
	60	0.609	27	0.019	0.143	3.1E-02	0.50
	80	0.629	22	0.018	0.140	2.3E-02	0.53
Naf-S-5	40	0.488	46	0.041	0.212	1.4E-03	-
	60	0.533	29	0.016	0.165	2.6E-02	0.36
	80	0.577	18	0.020	0.210	7.7E-03	0.60
Naf-C-2	40	0.544	32	0.020	0.264	4.3E-02	0.98
	60	0.567	30	0.018	0.223	4.4E-02	0.82
	80	0.671	24	0.023	0.234	7.6E-03	-

Table 5. Fit parameters for the V-i curves of Nano-composites membranes and Nafion® 212 membranes using 2M methanol solutions at different operation cell temperatures. Also in the table we give the methanol flux and $\chi \cdot J_{eos}$ (i.e.=A_3-L/σ) (V cm^2 mA^{-1}) parameters for the electro-osmotic diffusion of methanol across the membranes. The thickness considered for the membrane has been in wet conditions.

Membrane	***T*** **(ºC)**	σ **(S/cm)**	α	***A*** **(V)**	A_3 **($\Omega \cdot cm^2$)**	$\chi \cdot J_{eos}$ **$V \cdot cm^2 \cdot mA^{-1}$**
Nafion®	40	0.066	0.41	0.039	$10x10^{-4}$	$1.7x10^{-3}$
	60	0.073	0.94	0.017	$9x10^{-4}$	$1.6x10^{-3}$
	80	0.077	0.95	0.017	$8x10^{-4}$	$1.57x10^{-3}$
Naf-S-1	40	0.066	0.46	0.035	$11x10^{-4}$	$1.88x10^{-3}$
	60	0.073	0.85	0.019	$10x10^{-4}$	$1.70x10^{-3}$
	80	0.073	0.89	0.018	$9x10^{-4}$	$1.60x10^{-3}$
Naf-S-5	40	0.050	0.40	0.041	$13x10^{-4}$	$2.3x10^{-3}$
	60	0.066	0.80	0.016	$12x10^{-4}$	$2.1x10^{-3}$
	80	0.072	0.77	0.020	$11x10^{-4}$	$1.9x10^{-3}$
Naf-C-2	40	0.040	0.80	0.020	$18x10^{-4}$	$3.1x10^{-3}$
	60	0.047	0.89	0.018	$16x10^{-4}$	$2.7x10^{-3}$
	80	0.047	0.70	0.023	$13x10^{-4}$	$2.47x10^{-3}$

Figure Captions:

Figure 1: Schema of immersion modification process set-up.

Figure 2: Schema of crossover modification process set-up.

Figure 3: FTIR spectra of Nafion and all modified membranes a) spectral region between 600 at 4000 cm^{-1} and b) magnification between 1400 and 2000 cm^{-1}

Figure 4: Thermogravimetric analysis curves of Nafion, Naf-S-5 and Naf-C-4 recorded under air atmosphere at 10ºC/min. a) TGA and b) DTG

Figure 5: Representation of the minim square correlation slopes from methanol concentration versus time at the permeability experiments for Nafion and all modified membranes at: (a) 70ºC and (b) room temperature.

Figure 6: Left: Variation of the cell voltage, V, versus current density I for MEAs prepared with the composite membranes at different temperatures: (A) 40ºC, (B) 60ºC and (C) 80ºC. The methanol feed concentrations in all the experiments were 2M. Close symbols polarization curves and open symbols power density. The lines represent the best fit of the experimental data.

Figure 7. Fit of V-i curves using eq (6) for for Nafion® (■) and Naf-S-1 (●), Naf-S-5 (▲) and Naf-C-2 (▼) membranes. The lines represent the fit of experimental data..

Figure 8. Single cell voltage vs. current density between 100 and 300 mA/cm^2 for MEAs prepared from Nafion® (■), Naf-S-1 (■), Naf-S-5 (▲) and Naf-C-2 (▼) at 80 ºC and 2M methanol concentration of feed. The lines represent the fit to obtain the parameter A_3 using the eq.(12) and from them the parameter $\chi \cdot J_{eos}$ ($V \cdot cm^2 \cdot mA^{-1}$) for the electro-osmotic diffusion of methanol across the membranes.

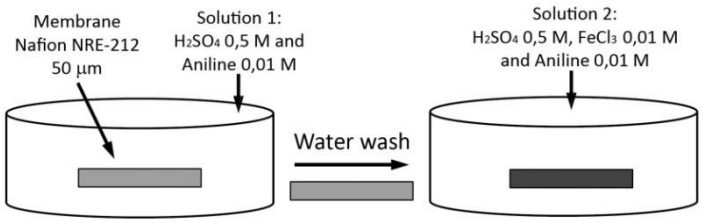

Figure 1: González-Ausejo et al.

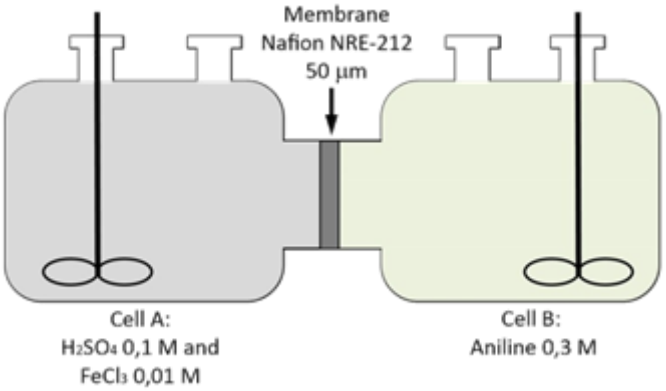

Figure 2: González-Ausejo et al.

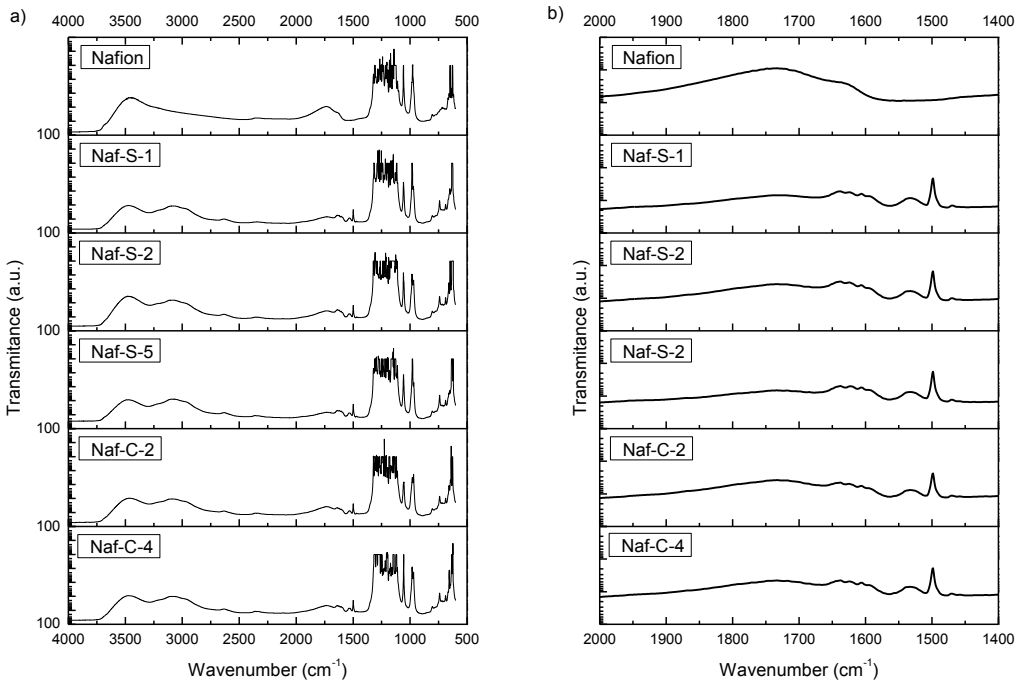

Figure 3: González-Ausejo et al.

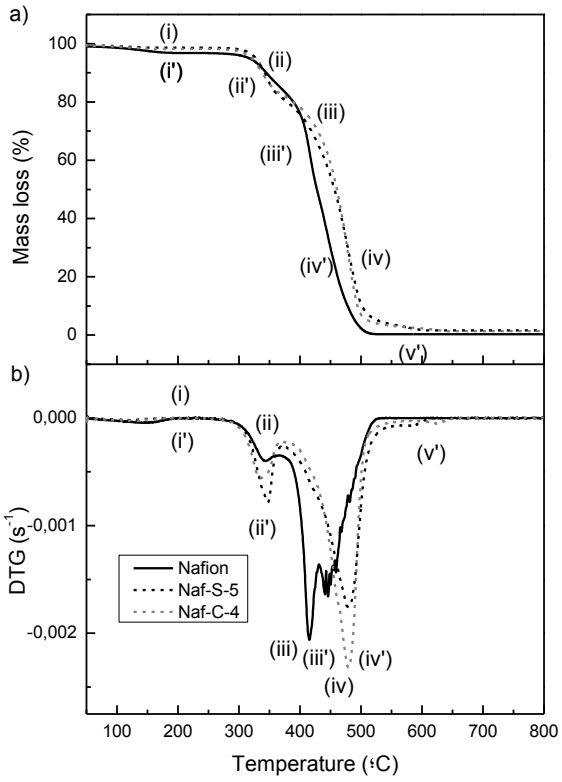

Figure 4: González-Ausejo et al.

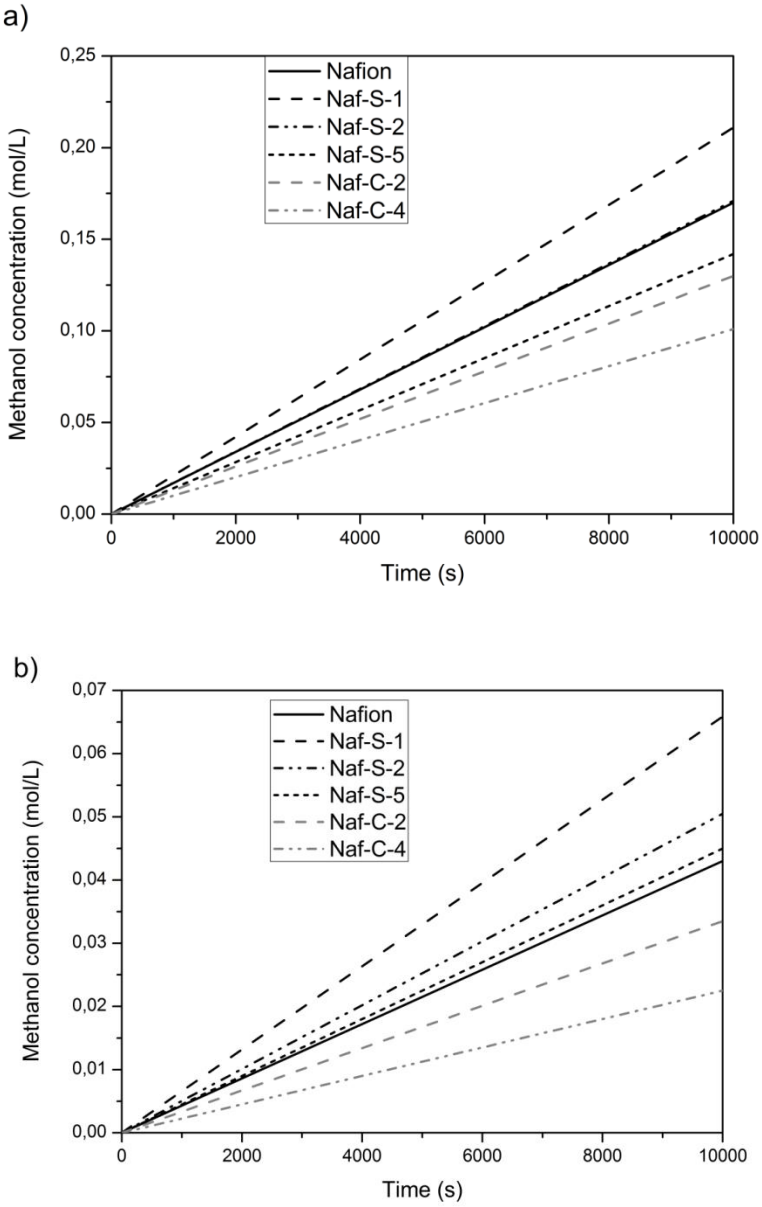

Figure 5: González-Ausejo et al.

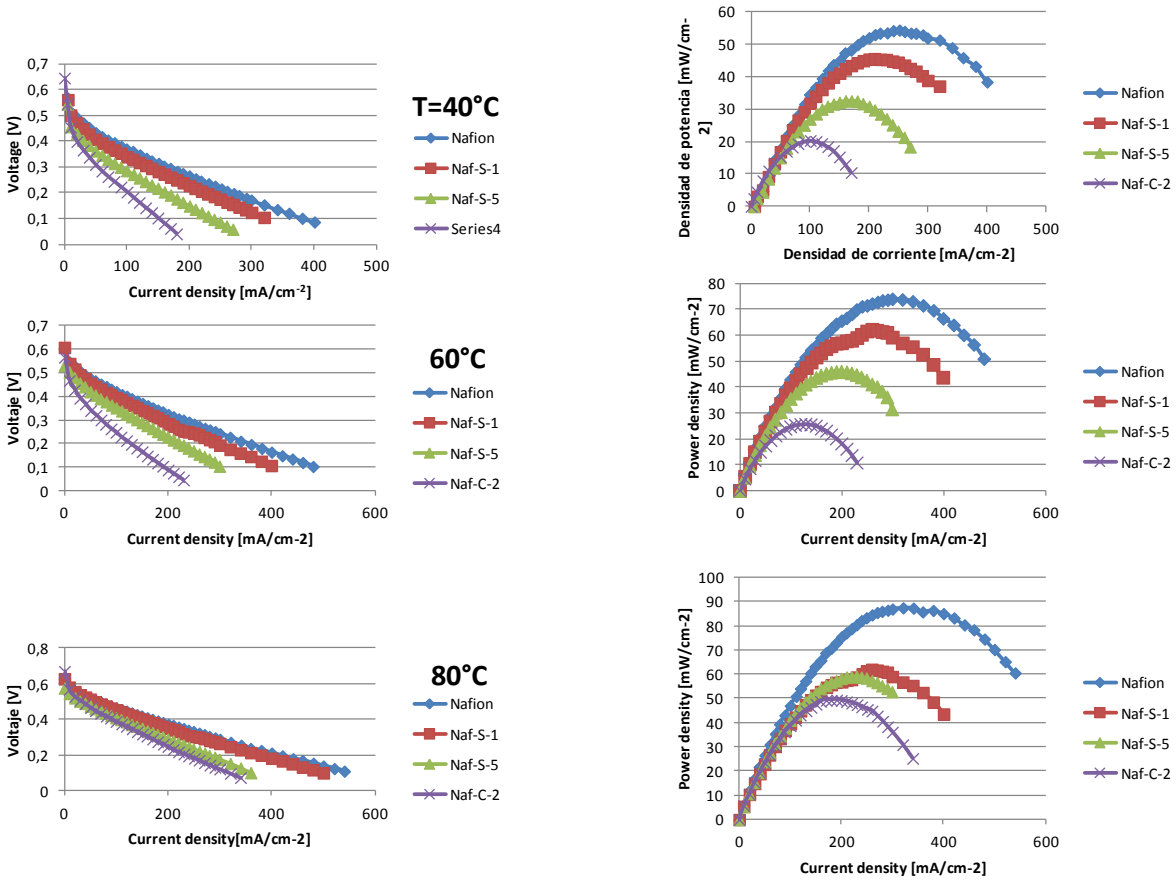

Figure 6: González-Ausejo et al.

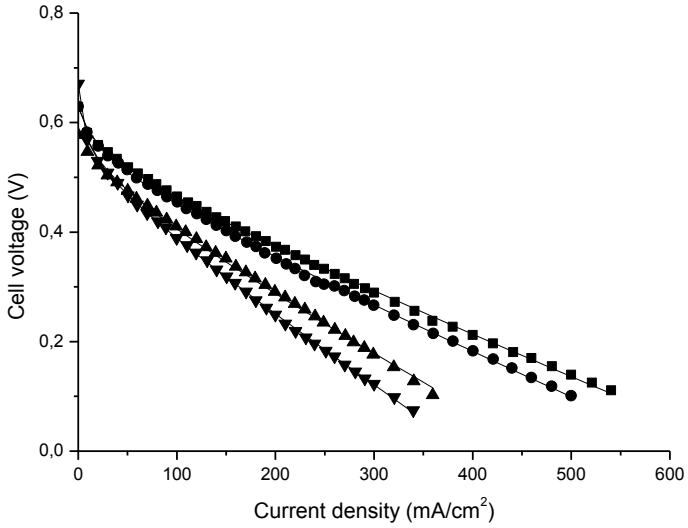

Figure 7: González-Ausejo et al.

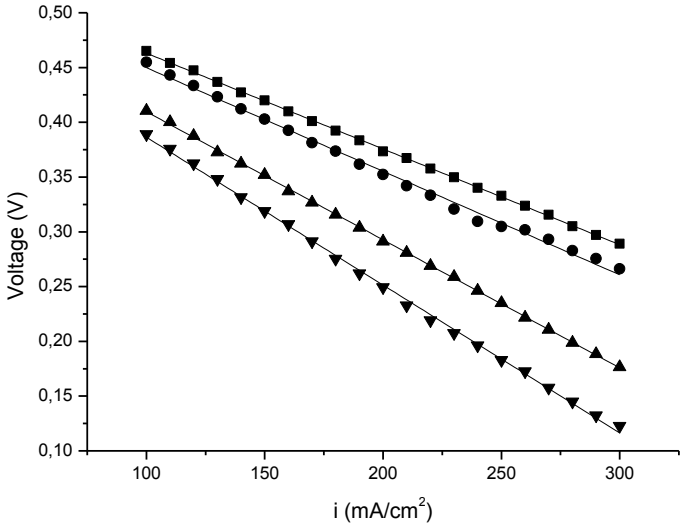

Figure 8: González-Ausejo et al.